Quantum dynamics of bosons in a two-ring ladder: Dynamical algebra, vortexlike excitations, and currents

Andrea Richaud and Vittorio Penna
Dipartimento di Scienza Applicata e Tecnologia and u.d.r. CNISM, Politecnico di Torino, Corso Duca degli Abruzzi 24, I-10129 Torino, Italy
(Received 14 April 2017; published 18 July 2017)

We study the quantum dynamics of the Bose-Hubbard model on a ladder formed by two rings coupled by the tunneling effect. By implementing the Bogoliubov approximation scheme, we prove that, despite the presence of the inter-ring coupling term, the Hamiltonian decouples in many independent sub-Hamiltonians $\hat{H}_k$ associated with momentum-mode pairs $\pm k$. Each sub-Hamiltonian $\hat{H}_k$ is then shown to be part of a specific dynamical algebra. The properties of the latter allow us to perform the diagonalization process, to find the energy spectrum and the conserved quantities of the model, and to derive the time evolution of important physical observables. We then apply this solution scheme to the simplest possible closed ladder, the double trimer. After observing that the excitations of the system are weakly populated vortices, we explore the corresponding dynamics by varying the initial conditions and the model parameters. Finally, we show that the inter-ring tunneling determines a spectral collapse when approaching the border of the dynamical-stability region.

DOI: 10.1103/PhysRevA.96.013620

I. INTRODUCTION

Recent advances in ultracold atom physics have made it possible to study a wide range of many-body quantum systems of fermions, bosons, and even mixtures of two atomic species. The phenomenology one can explore is so rich that a new area of investigation, which goes by the name of atomtronics, has emerged [1]. A system of ultracold atoms subject to a spatially periodic potential features a band diagram which is conceptually equivalent to those relevant to electrons in standard crystal lattices. It is therefore possible to engineer ultracold-atom equivalents of the usual electronic materials, i.e., conductors, dielectrics, and semiconductors [2]. Properly tailoring the periodic optical potential, one can achieve behaviors similar to doped semiconductors. The latter can be used to realize the atomtronic counterpart of traditional electron devices, such as diodes and bipolar junction transistors [3], which, in turn, can be used as building blocks for actual circuits, such as amplifiers, flip flops, and logic gates [4,5].

In parallel, systems of ultracold neutral atoms have been used to simulate interesting many-body phenomena in their most simple and essential forms, avoiding the complications usually encountered in actual materials [6,7]. The charge neutrality of these systems does not prevent the observation of the interesting phenomena characterizing charged particles in a magnetic field. For example, the equivalence between the Lorentz and the Coriolis forces allows one to realize synthetic magnetic fields in *rotating* systems of neutral particles [8]. Also, the current cutting-edge technologies have enabled the detection of bosonic chiral currents in ladders [9] and the study of quantum transport in ultracold gases in optical lattices [10] and of topological quantum matter [11].

In this work we focus on a specific lattice geometry, the Bose-Hubbard ladder with periodic boundary conditions. This kind of system was designed in [12] for a single ring and in [13] for a ladder and has attracted increasing attention in recent years. It consists of two vertically stacked rings whose sites are populated by weakly interacting bosons. The current dynamics in a two-ring system subject to a synthetic magnetic field was studied in [13] in the weak-coupling regime by means of two-mode Gross-Pitaevskii equations. The same mean-field approach has been used to study angular momentum Josephson oscillations [14] and the coherent transfer of vortices [15], while persistent currents flowing in the two-ring system have been demonstrated [16] to provide a physical implementation of a qubit. The effect of an artificial magnetic field on an open ladder was investigated in [17] and, more recently, in [18,19]. These studies have shown that this lattice geometry leads to the one-dimensional equivalent of a vortex lattice in a superconductor and that a true Meissner-to-vortex transition occurs at a certain critical field. Finally, [20] presented a field-theoretical approach for the determination of the ground state, while different possible currents regimes were studied in [21,22]. Recently, the presence of the Meissner effect was observed in the bosonic ladder [9], while the phase diagram thereof was discussed in [23].

Motivated by the considerable interest in coupled annular Bose-Einstein condensates in recent years, in this paper we investigate the two-ring ladder from a different perspective, with the aim of giving accurate insight into its quantum dynamics. We move from the site-mode picture (where the expectation values of operators are local order parameters of the lattice sites) to the momentum-mode picture (where expectation values of operators are collective order parameters in momentum space). In the momentum domain, we perform the well-known Bogoliubov approximation under the assumption that in both rings the same momentum mode r is macroscopically occupied. The ensuing model Hamiltonian is shown to decouple into many sub-Hamiltonians $\hat{H}_k$, one for each *pair* of momentum modes. Each sub-Hamiltonian $\hat{H}_k$ is proved to belong to the dynamical Lie algebra so(2,3).

The recognition of a certain dynamical algebra, together with its invariants, has been used to find the spectrum and the time evolution of quantum systems [24–31] and, once again, has proved to be the key element for the analytic solution of the model under scrutiny. The remarkable importance of this abstract mathematical property is that it provides an effective diagonalization scheme and helps us to find conserved quantities. Moreover, the time evolution of several

meaningful observables belonging to the dynamical algebra can be obtained by solving a linear system of differential equations.

In Sec. II, we present the Bose-Hubbard (BH) Hamiltonian associated with the two-ring ladder and implement the Bogoliubov scheme. In Sec. III, we prove that the model Hamiltonian belongs to a dynamical algebra, namely, so(2,3). We show that the algebra Casimir invariant correctly corresponds to angular momentum, and we find the excitation spectrum. In Sec. IV, we apply this solution scheme to the simplest possible closed ladder, the double trimer. Moreover, we show that the excitations of the system correspond to weakly populated vortices, we derive the time evolution of some physical observables commonly studied in the literature, and we describe various significant quantum processes that occur in the system. In Sec. V, we explore the dynamics of excited bosons by varying the initial conditions and the model parameters, emphasizing the role played by initial phase differences. We also comment on the fact that properly choosing certain parameters, the system can approach dynamical instability. In particular, we show how a spectral collapse takes place when the inter-ring tunneling reaches a specific critical value. Section VI is devoted to concluding remarks.

II. MODEL PRESENTATION

In this section we reformulate the BH Hamiltonian describing the ladder system and including the inter-ring tunneling term by means of momentum modes characterizing the Bogoliubov picture.

A. Site-mode picture

The second-quantized Hamiltonian describing bosons confined in a two-ring ladder is

$$\begin{aligned}\hat{H} = &-T_a\sum_{j=1}^{M_s}(A_{j+1}^\dagger A_j + A_j^\dagger A_{j+1}) + \frac{U_a}{2}\sum_{j=1}^{M_s} N_j(N_j-1)\\ &- T_b\sum_{j=1}^{M_s}(B_{j+1}^\dagger B_j + B_j^\dagger B_{j+1}) + \frac{U_b}{2}\sum_{j=1}^{M_s} M_j(M_j-1)\\ &- T\sum_{j=1}^{M_s}(A_jB_j^\dagger + B_jA_j^\dagger). \end{aligned} \tag{1}$$

One can recognize two *intra-ring* tunneling terms (T_a and T_b), two on-site repulsive terms (U_a and U_b), and an *inter-ring* tunneling term T. These site operators satisfy standard bosonic commutators: $[A_j,A_k^\dagger]=\delta_{j,k}$, $[B_j,B_k^\dagger]=\delta_{j,k}$, while $[A_j,B_k^\dagger]=0$. $N_j=A_j^\dagger A_j$ and $M_j=B_j^\dagger B_j$ are number operators. The number of lattice sites in each ring is denoted by M_s.

B. Momentum-mode picture

Due to the ring structure of the system, it is convenient to introduce momentum-mode operators a_k and b_k, whose relation to the site operator is

$$A_j=\sum_{k=1}^{M_s}\frac{a_k}{\sqrt{M_s}}e^{+i\tilde{k}aj},\quad B_j=\sum_{k=1}^{M_s}\frac{b_k}{\sqrt{M_s}}e^{+i\tilde{k}aj},$$

with $\tilde{k}=\frac{2\pi}{L}k$ and $L=M_sa$. The length a is the intersite distance, L is the ring circumference, and the summations run on the first Brillouin zone. Notice that the use of the momentum-mode picture is justified by the fact that we are considering a *repulsive* on-site interaction $U>0$, which, in turn, is linked to a ground state where bosons are delocalized in the system. Momentum-mode operators a_k and b_k inherit bosonic commutation relations: $[a_j,a_k^\dagger]=\delta_{j,k}$, $[b_j,b_k^\dagger]=\delta_{j,k}$, and $[a_j,b_k^\dagger]=0$. Number operators $n_k=a_k^\dagger a_k$ and $m_k=b_k^\dagger b_k$ count the number of bosons having (angular) momentum $\hbar k$. In this new picture, the Hamiltonian can be written as

$$\begin{aligned}\hat{H} = &\frac{U_a}{2M_s}\sum_{p,q,k=1}^{M_s} a_{q+k}^\dagger a_{p-k}^\dagger a_q a_p - 2T_a\sum_{k=1}^{M_s} a_k^\dagger a_k\cos(a\tilde{k})\\ &+\frac{U_b}{2M_s}\sum_{p,q,k=1}^{M_s} b_{q+k}^\dagger b_{p-k}^\dagger b_q b_p - 2T_b\sum_{k=1}^{M_s} b_k^\dagger b_k\cos(a\tilde{k})\\ &- T\sum_{k=1}^{M_s}(a_kb_k^\dagger + a_k^\dagger b_k).\end{aligned}$$

Let us assume that, in both rings, momentum mode r is macroscopically occupied. Further, for the sake of simplicity, we assume M_s is an odd (positive) integer. Under the hypothesis that the condensate is weakly interacting (small U/T) and thus is in the superfluid region of the BH phase diagram, it is possible to perform the well-known Bogoliubov approximation [32,33] (see Appendix A for details). We observe that this scheme can be applied as well in the case $U<0$, describing attractive bosons, provided the ratio $|U|/T$ is small enough. This condition guarantees that bosons are delocalized and superfluid [34]. One thus discovers that the Hamiltonian, apart from a constant term, decouples in $(M_s-1)/2$ independent Hamiltonians $\hat{H}_k$, one for each *pair* of momentum modes,

$$\hat{H}=E_0+\sum_{k>0}\hat{H}_k, \tag{2}$$

where $E_0=u_a(N-1)/2+u_b(M-1)/2-2\cos(a\tilde{r})(T_aN+T_bM)-2T\sqrt{NM}$ is the ground-state energy, and

$$\begin{aligned}\hat{H}_k = &\,2\sin(a\tilde{r})\sin(a\tilde{k})[T_a(n_{r+k}-n_{r-k})\\ &+T_b(m_{r+k}-m_{r-k})]\\ &+\gamma_{a,k}(n_{r+k}+n_{r-k})+u_a(a_{r+k}^\dagger a_{r-k}^\dagger + a_{r+k}a_{r-k})\\ &+\gamma_{b,k}(m_{r+k}+m_{r-k})+u_b(b_{r+k}^\dagger b_{r-k}^\dagger + b_{r+k}b_{r-k})\\ &-T(a_{r+k}b_{r+k}^\dagger + a_{r+k}^\dagger b_{r+k} + a_{r-k}b_{r-k}^\dagger + a_{r-k}^\dagger b_{r-k}).\end{aligned}$$

The parameters

$$\gamma_{a,k} = -2T_a \cos(a\tilde{r})(\cos(a\tilde{k}) - 1) + u_a - T\sqrt{\frac{M}{N}},$$
$$\gamma_{b,k} = -2T_b \cos(a\tilde{r})(\cos(a\tilde{k}) - 1) + u_b - T\sqrt{\frac{N}{M}},$$
$$u_a = \frac{U_a N}{M_s}, \quad u_b = \frac{U_b M}{M_s},$$

have been introduced to simplify the notation, and N and M are the total numbers of bosons in the two rings. If $T_a = T_b = T_\parallel$, the whole term

$$2\sin(a\tilde{r})\sin(a\tilde{k})T_\parallel(n_{r+k} - n_{r-k} + m_{r+k} - m_{r-k}) \quad (3)$$

can be shown (see Sec. III) to be a constant of motion and thus can be incorporated into E_0. The natural basis of the Hilbert space relevant to model Hamiltonian $\hat{H}_k$ is $\{|n_{r+k}, n_{r-k}, m_{r+k}, m_{r-k}\rangle\}$, a basis vector being labeled by *four* momentum quantum numbers. In regard to the values n_0 and m_0, due to the Bogoliubov approach, they inherently depend on $n_{r\pm k}$ and $m_{r\pm k}$, their expressions being $n_0 = N - \sum_k (n_{r+k} + n_{r-k})$ and $m_0 = M - \sum_k (m_{r+k} + m_{r-k})$.

III. DYNAMICAL ALGEBRA

In general, a dynamical algebra $\mathcal{A}$ is a Lie algebra, i.e., n-dimensional vector space spanned by n generators (operators) $\hat{e}_1, \hat{e}_2, \ldots, \hat{e}_n$ closed under commutation. The closure property means that the commutator of any two algebra elements is again an algebra element. A Lie algebra is univocally specified once all the commutators $[\hat{e}_j, \hat{e}_k] = i\sum_m f_{jkm}\hat{e}_m$ are given, namely, when the set of the so-called structure constants $\{f_{jkm}\}$ is specified [25]. A model Hamiltonian $\hat{H}$ belongs to a dynamical algebra $\mathcal{A} = \text{span}\{\hat{e}_1, \hat{e}_2, \ldots, \hat{e}_n\}$ whenever $\hat{H}$ can be expressed as a linear combination $\hat{H} = \sum_j h_j \hat{e}_j$ of the generators of $\mathcal{A}$. The important consequences of this property are that (a) conserved physical quantities correspond to the algebra's invariants, (b) the diagonalization process of $\hat{H}_k$ becomes straightforward, and (c) the Heisenberg equations can be shown to form a simple linear system of differential equations. Under the assumption $T_a = T_b = T_\parallel$, Hamiltonian $\hat{H}_k$ is recognized to be an element of the dynamical algebra $\mathcal{A} = \text{so}(2,3)$, a ten-dimensional Lie algebra spanned by the operators

$$A_+ = a^\dagger_{r+k}a^\dagger_{r-k}, \quad B_+ = b^\dagger_{r+k}b^\dagger_{r-k},$$
$$A_- = (A_+)^\dagger, \quad B_- = (B_+)^\dagger,$$
$$A_3 = \frac{n_{r+k} + n_{r-k} + 1}{2}, \quad B_3 = \frac{m_{r+k} + m_{r-k} + 1}{2},$$
$$S_+ = a^\dagger_{r+k}b_{r+k} + a^\dagger_{r-k}b_{r-k}, \quad S_- = (S_+)^\dagger,$$
$$K_+ = a^\dagger_{r-k}b^\dagger_{r+k} + a^\dagger_{r+k}b^\dagger_{r-k}, \quad K_- = (K_+)^\dagger. \quad (4)$$

One can easily see that $\hat{H}_k$, up to an inessential constant quantity $-\sum_{k>0}(\gamma_{a,k} + \gamma_{b,k})$, can be written as

$$\hat{H}_k = 2\gamma_{a,k}A_3 + u_a(A_+ + A_-) + 2\gamma_{b,k}B_3 + u_b(B_+ + B_-) - T(S_+ + S_-),$$

where operators $\{A_+, A_-, A_3\}$, associated with ring A, generate a su(1,1) algebra marked by the well-known commutators $[A_+, A_-] = -2A_3$, $[A_3, A_\pm] = \pm A_\pm$, and operators $\{B_+, B_-, B_3\}$, relevant to ring B, feature the same su(1,1) structure (an application of this dynamical algebra can be found in [35] for a trapped condensate).

However, the important term in $\hat{H}_k$ is the inter-ring tunneling term, which is responsible for an algebraic structure considerably more complex than the simple direct sum of two su(1,1) algebras. In Appendix B, the commutators of $A_\pm$, $B_\pm$, A_3, B_3, $K_\pm$, and $S_\pm$ are explicitly calculated, showing that, indeed, they do form the algebra so(2,3).

A. The algebra invariant as a constant of motion

In the absence of the inter-ring tunneling term, i.e., if T is zero, the two rings decouple and $\hat{H}_k$ could be seen as an element of the direct sum of two commuting algebras su(1,1). In such a case, the difference between the number of bosons having momentum $r + k$ and the number of bosons having momentum $r - k$ is a conserved quantity in each single ring. This statement can be easily proved by using the Casimir operator of the algebra su(1,1) for ring A,

$$C_a = A_3^2 - \tfrac{1}{2}(A_+A_- + A_-A_+) = A_4(A_4 + 1),$$

where

$$A_4 = \frac{n_{r+k} - n_{r-k} - 1}{2}.$$

We recall that, by definition, the Casimir operator (or, equivalently, A_4) commutes with all the algebra generators $A_\pm$, A_3. The same comment holds for Casimir operator C_b of $B_\pm$ and B_3.

Conversely, in the presence of the inter-ring tunneling term, neither $n_{r+k} - n_{r-k}$ nor $m_{r+k} - m_{r-k}$ represents conserved quantities any longer. Nevertheless, by applying the general recipe described in [36], one discovers that the Casimir operator of $\mathcal{A} = \text{so}(2,3)$ is

$$C = C_a + C_b + \frac{S_+S_- + S_-S_+}{4} - \frac{K_+K_- + K_-K_+}{4}.$$

This operator, a quadratic form involving all the algebra elements, can be rewritten in the standard form

$$C = C_4(C_4 + 2),$$

where

$$C_4 = \frac{n_{r+k} - n_{r-k} + m_{r+k} - m_{r-k}}{2} - 1.$$

The conserved quantity $L_z(k) = n_{r+k} - n_{r-k} + m_{r+k} - m_{r-k}$ has a nice physical interpretation. Apart from the inessential additive constant -1, C_4 is proportional to the difference between the numbers of bosons having momentum $r + k$ and momentum $r - k$ in the whole ring ladder. Then $L_z(k)$ can be interpreted as the angular momentum for the modes $r \pm k$. This fact not only proves the ansatz on the constant of motion (3) but, since it holds for every sub-Hamiltonian $\hat{H}_k$, leads to the natural conclusion that the angular momentum $L_z = \sum_{k>0} L_z(k)$ of the whole system is a conserved quantity. In this regard, it is worth noting that the ten operators which

generate the algebra so(2,3) always correspond to two-boson processes in which angular momentum is conserved.

B. Spectrum and diagonalization

Once the dynamical algebra has been identified, the Hamiltonian $\hat{H}_k$ can be diagonalized thanks to a simple unitary transformation U of group SO(2,3) defined as

$$U = e^{\frac{\varphi}{2}(S_- - S_+)} e^{\frac{\xi}{2}(K_- - K_+)} e^{\frac{\theta_a}{2}(A_- - A_+)} e^{\frac{\theta_b}{2}(B_- - B_+)}.$$

This represents the central step of the dynamical-algebra method. A suitable choice of parameters φ, ξ, θ_a, and θ_b, (see Appendix C for their explicit expressions) allows us to write the Hamiltonian

$$\hat{\mathcal{H}}_k = U^{-1}\,\hat{H}_k\,U = [c_1\cosh\theta_a - c_2\sinh\theta_a]A_3 + [c_3\cosh\theta_b - c_4\sinh\theta_b]B_3$$

as a linear combination of A_3 and B_3, operators which are *diagonal* in the Fock-state basis. The explicit expression of coefficients c_1, c_2, c_3, and c_4 is given in Appendix C, showing that they are complex functions of the interaction and the tunneling parameters. Based on the definitions (4), the spectrum of Hamiltonian $\hat{H}_k$ is found to be

$$E_k(n_{r+k},n_{r-k},m_{r+k},m_{r-k}) = +[c_1\cosh\theta_a - c_2\sinh\theta_a]\frac{n_{r+k}+n_{r-k}+1}{2} + [c_3\cosh\theta_b - c_4\sinh\theta_b]\frac{m_{r+k}+m_{r-k}+1}{2},$$

where $n_{r\pm k}$ and $m_{r\pm k}$ now represent the quantum numbers describing the boson populations.

C. The time evolution of algebra elements

The knowledge of the dynamical algebra $\mathcal{A}$ relevant to a given model Hamiltonian $\hat{H} = \sum_j h_j\hat{e}_j$ allows one to derive in a direct way the equations of motion of any physical observable $\mathcal{O} = \sum_k o_k\hat{e}_k$ written in terms of the generators $\hat{e}_k \in \mathcal{A}$. If $[\hat{e}_j,\hat{e}_k] = i\sum_m f_{jkm}\hat{e}_m$ represent the commutators of $\mathcal{A}$ (f_{jkm} are the algebra structure constants), then the Heisenberg equation for $\hat{e}_k$ reduces to a simple linear combination of the generators,

$$i\hbar\frac{d}{dt}\hat{e}_k = [\hat{e}_k,\hat{H}] = i\sum_m \rho_{km}\hat{e}_m,$$

where $\rho_{km} = \sum_j h_j f_{jkm}$ and the commutators have been used to explicitly calculate $[\hat{e}_k,\hat{H}]$. The dynamical evolution of the whole system is thus encoded in a simple set of linear equations whose closed form is ensured by the commutators of the dynamical algebra and whose number corresponds to the algebra dimension. The evolution of physical observables $\mathcal{O}$ is thus fully determined by that of generators $\hat{e}_k$.

Concerning the dynamical algebra so(2,3), the linear system of differential equations is

$$\begin{aligned}
i\hbar\dot{A}_3 &= u_a(A_+ - A_-) - T\left(\frac{1}{2}S_+ - \frac{1}{2}S_-\right),\\
i\hbar\dot{A}_- &= 2\gamma_{a,k}A_- + 2u_aA_3 - TK_-,\\
i\hbar\dot{B}_3 &= u_b(B_+ - B_-) - T\left(-\frac{1}{2}S_+ + \frac{1}{2}S_-\right),\\
i\hbar\dot{B}_- &= 2\gamma_{b,k}B_- + 2u_bB_3 - TK_-,\\
i\hbar\dot{S}_- &= \gamma_{a,k}S_- + u_aK_+ - \gamma_{b,k}S_- - u_bK_- + 2T(A_3 - B_3),\\
i\hbar\dot{K}_- &= \gamma_{a,k}K_- + u_aS_+ + \gamma_{b,k}K_- + u_bS_- - 2T(A_- + B_-).
\end{aligned}$$

Of course, the remaining four equations for A_+, B_+, S_+, and K_+ are the Hermitian conjugates of the Heisenberg equations for A_-, B_-, S_-, and K_-. Rigorously, this is a system of *operator* ordinary differential equations (ODEs), as the unknowns are the time evolution of operators. In the following we will switch from operators to their expectation values, i.e., from operator ODEs to standard complex ODEs. In fact the structure of Heisenberg equations remains unchanged when taking the expectation values on both sides, e.g.,

$$i\hbar\frac{d}{dt}\langle A_3\rangle = u_a(\langle A_+\rangle - \langle A_-\rangle) - T\left(\frac{1}{2}\langle S_+\rangle - \frac{1}{2}\langle S_-\rangle\right).$$

This conceptual jump will often be made and always understood throughout this paper.

IV. DOUBLE TRIMER

The formulas we have presented so far are very general because they can capture the dynamics of physical regimes distinguished by an arbitrary macroscopic mode r with $0 \leqslant r \leqslant M_s - 1$ and an arbitrary choice of the site number M_s and of the other model parameters. In particular, for $r \neq 0$, our approach allows us to investigate the dynamics of quantum excitations relevant to the macroscopic (semiclassical) double-vortex state characterized by a total vorticity proportional to r,

$$A_j(t,r) = \sqrt{\frac{N}{M_s}}e^{ij\tilde{r}-\omega_r t}, \quad B_j(t,r) = \sqrt{\frac{M}{M_s}}e^{ij\tilde{r}-\omega_r t},$$

where A_j, B_j are the local order parameters (of the semiclassical Hamiltonian) associated with model (1) and ω_r can be found with the corresponding dynamical equations [37]. In this section we show a simple and yet very interesting application of the solution scheme we have proposed. We consider the smallest possible ladder, the one formed by two rings with $M_s = 3$ sites (trimer). This system has received considerable attention in the last decade in that it represents the minimal circuit in which chaos can be triggered [38–40]. Moreover, we assume that the macroscopically occupied mode is $r = 0$ (entailing that no macroscopic current is present), that the upper and lower rings host an equal number of bosons ($N = M$), and that the intra-ring tunneling and the on-site repulsion parameters are equal ($T_a = T_b =: T_\parallel$ and $U_a = U_b =: U$). As a consequence, $\gamma_{a,k} = \gamma_{b,k} = \gamma_k$. Since the first Brillouin zone involves just three modes, $k = -1, 0, 1$, then there is only one γ_k, which will be denoted by

$$\gamma = \gamma_1 = 2T_\parallel\left[1 - \cos\left(\frac{2\pi}{3}\right)\right] + u - T.$$

By performing the Bogoliubov approximation with the momentum mode $r = 0$ macroscopically occupied, the double-trimer Hamiltonian can be written as $\hat{H} = E_0 + \hat{H}_1$, where

$$\begin{aligned}
E_0 &= u(N-1) - 2N(2T_\parallel + T) - 2\gamma,\\
\hat{H}_1 &= 2\gamma(A_3 + B_3) + u(A_+ + A_- + B_+ + B_-)\\
&\quad - T(S_+ + S_-).
\end{aligned}$$

Notice that E_0 is a constant quantity, while $\hat{H}_1$ rules the dynamics of bosons having wave-number $k = \pm 1$.

As we proved in the previous section, the total angular momentum, which is proportional to $n_1 - n_{-1} + m_1 - m_{-1}$, is a conserved quantity. In passing, we note that for a double trimer with twin rings ($\gamma_a = \gamma_b, u_a = u_b$), a second quantity commuting with Hamiltonian $\hat{H}_1$,

$$I = (a_1 b_1^\dagger + a_1^\dagger b_1) - (a_{-1} b_{-1}^\dagger + a_{-1}^\dagger b_{-1}),$$

can be found. In view of the mode coupling characterizing the hopping term of a BH model, I can be interpreted as the difference between the tunneling energies associated with the ring-ring boson exchange for the bosons of mode $k = 1$ and the bosons of mode $k = -1$.

Concerning the diagonalization of $\hat{H}_1$, generalized rotation angles φ, ξ, θ_a, and θ_b are, in such a system,

$$\varphi = \frac{\pi}{2}, \quad \xi = 0, \quad \tanh\theta_a = \frac{u}{\gamma - T}, \quad \tanh\theta_b = \frac{u}{\gamma + T}. \tag{5}$$

They lead to the diagonal Hamiltonian

$$\hat{\mathcal{H}} = E_0 + 2\hbar\omega\, A_3 + 2\hbar\Omega\, B_3, \tag{6}$$

where the two frequencies

$$\omega = \frac{\sqrt{3T_\parallel(3T_\parallel + 2u)}}{\hbar}, \tag{7}$$

$$\Omega = \frac{\sqrt{(3T_\parallel - 2T)(3T_\parallel - 2T + 2u)}}{\hbar} \tag{8}$$

have been defined. Since $A_3 = (n_k + n_{-k} + 1)/2$ and $B_3 = (m_k + m_{-k} + 1)/2$, then $\hat{\mathcal{H}}$ formally corresponds to a system of four independent harmonic oscillators with the spectrum $E_k(n_k,n_{-k},m_k,m_{-k}) = E_0 + \hbar\omega(n_k + n_{-k} + 1) + \hbar\Omega(m_k + m_{-k} + 1)$. The angle θ_a and the argument of the square roots are well defined only in a certain region of the three-dimensional parameter space $(T_\parallel, U, T)$. From a dynamical point of view, approaching the border of this *stability region* implies that the system tends to be unstable and many physical quantities manifest diverging behaviors. This issue will be addressed in Sec. V.

A. Vortexlike excitations and currents

It is interesting to notice that the weak excitations in each ring are weakly populated vortices. To show this, let us observe that, in the semiclassical picture, site-mode operators corresponding to momentum-mode operators $a_0 = \sqrt{N - n_1 - n_{-1}}, a_1 = \sqrt{n_1}e^{i\phi_1}, a_{-1} = \sqrt{n_{-1}}e^{i\phi_{-1}}$ are

$$A_j = \frac{1}{\sqrt{3}}\left[\sqrt{n_0} + e^{+i\frac{2\pi}{3}j}\sqrt{n_{-1}}e^{i\phi_{-1}} + e^{-i\frac{2\pi}{3}j}\sqrt{n_1}e^{i\phi_1}\right],$$

where $n_0 = N - n_{-1} - n_1$ and $j = 1,2,3$ is the site index. The structure of site operators A_j, whose expectation values are the local order parameters, clearly shows that the state of the system is the superposition of three contributions, namely, a major mode a_0 corresponding to a zero supercurrent and two minor modes (a_1 and a_{-1}) corresponding to counter-rotating weakly populated vortices. The same holds also for site-mode operators B_j of ring B.

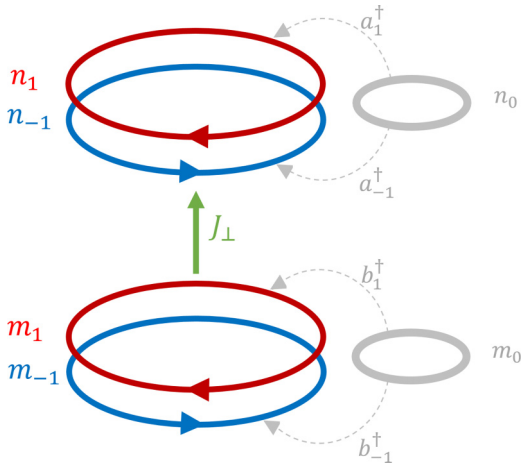

FIG. 1. Schematic representation of the vortexlike weak excitations in our system. In each ring there can be both a clockwise current and an anticlockwise current. $J_\perp$ denotes the current of excited bosons between the two rings. The macroscopically occupied modes n_0 and m_0 (in gray), being semiclassic, can be considered a sort of reservoir.

Let us introduce some observables, commonly found in the literature (see for example [18,41]), whose time evolution allows one to illustrate the significant transport phenomena and inter-ring exchange processes occurring in the system. We start with the currents along the two rings,

$$J_A = iT_\parallel \sum_{l=1}^{3}(A_{l+1}^\dagger A_l - A_l^\dagger A_{l+1}) = \sqrt{3}T_\parallel(n_1 - n_{-1}),$$

$$J_B = iT_\parallel \sum_{l=1}^{3}(B_{l+1}^\dagger B_l - B_l^\dagger B_{l+1}) = \sqrt{3}T_\parallel(m_1 - m_{-1}).$$

These currents are proportional to the angular momenta in each single ring. Their superposition $J_{\rm tot} = J_A + J_B$ is proportional to the total angular momentum (and thus is a conserved quantity), while $J_{\rm chir} = J_A - J_B$ is proportional to the angular momentum difference between the two rings. $N_* = n_1 + n_{-1} + m_1 + m_{-1}$ is the total number of excited bosons. The rung excitations' current

$$J_\perp = iT\sum_{l=1}^{3}(A_l^\dagger B_l - B_l^\dagger A_l)$$
$$= iT(a_1^\dagger b_1 + a_{-1}^\dagger b_{-1} - a_1 b_1^\dagger - a_{-1} b_{-1}^\dagger)$$

measures the flow of excited bosons from ring B to ring A. Figure 1 sketches the scenario of physical observables which come into play.

B. Time evolution of observables and dynamical algebra

Based on the scheme described in Sec. III C, the dynamical algebra so(2,3) allows one to determine the equations of motion for the total number of excited bosons N_* and for the rung current $J_\perp$. Since these two observables can be written as linear combinations of the so(2,3) generators, it is possible to write their dynamical equations in terms of algebra elements. Concerning N_*, the corresponding Heisenberg equation is

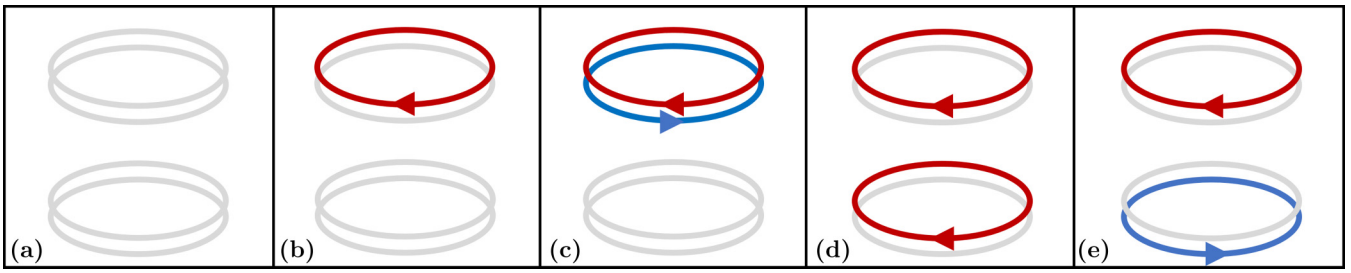

FIG. 2. Five different initial conditions. (a) No initial excitations, (b) a weak vortex in one ring, (c) a pair of counter-rotating weak vortices in the same ring, (d) two equal weak vortices in the two rings, and (e) a pair of counter-rotating weak vortices in the two rings.

found to be

$$\frac{dN_*}{dt} = 2(\dot{A}_3 + \dot{B}_3) = -\frac{2u}{\hbar} i(A_+ - A_- + B_+ - B_-).$$

Recalling that $A_+ - A_- + B_+ - B_- = a_1^\dagger a_{-1}^\dagger - a_1 a_{-1} + b_1^\dagger b_{-1}^\dagger - b_1 b_{-1}$, this equation shows that the time variation of N_* is proportional to a generalized current which can be interpreted as the boson pairs flow from the macroscopically occupied modes a_0 and b_0 to the excited modes. In other words, this is the generation rate of boson pairs populating modes $k = \pm 1$. Such a pair is created by $a_1^\dagger a_{-1}^\dagger$ (annihilated by $a_1 a_{-1}$) extracting (releasing) bosons from (to) the macroscopically occupied modes which, being semiclassical, have bowed out and act as reservoirs (see Fig. 1).

In regard to the rung current, the relevant Heisenberg equation reads

$$\frac{d}{dt} j_\perp = iT(\dot{S}_+ - \dot{S}_-) = \frac{-4T^2}{\hbar}(A_3 - B_3)$$
$$= \frac{-2T^2}{\hbar}(n_1 + n_{-1} - m_1 - m_{-1}),$$

showing that a population imbalance between the two rings is responsible for the time variation of the rung current.

If one is interested in obtaining finer-grained information about the system, e.g., finding the time evolution of a certain population $n_{\pm 1}$ or $m_{\pm 1}$, one must consider an enlarged dynamical algebra containing the original framework so(2,3). This is represented by the 15-dimensional algebra so(2,4), which, in fact, includes the 10-dimensional algebra so(2,3). It is within this enlarged algebra (whose generators are listed in Appendix D) that the dynamics of all the previously presented observables can be represented. The time evolution of excited populations is easily found to be

$$i\hbar \dot{n}_1 = u(a_1^\dagger a_{-1}^\dagger - a_1 a_{-1}) - T(-a_1 b_1^\dagger + a_1^\dagger b_1),$$
$$i\hbar \dot{n}_{-1} = u(a_1^\dagger a_{-1}^\dagger - a_1 a_{-1}) - T(-a_{-1} b_{-1}^\dagger + a_{-1}^\dagger b_{-1}),$$
$$i\hbar \dot{m}_1 = u(b_1^\dagger b_{-1}^\dagger - b_1 b_{-1}) - T(a_1 b_1^\dagger - a_1^\dagger b_1),$$
$$i\hbar \dot{m}_{-1} = u(b_1^\dagger b_{-1}^\dagger - b_1 b_{-1}) - T(a_{-1} b_{-1}^\dagger - a_{-1}^\dagger b_{-1}).$$

These equations clearly show that the time evolution of excited populations can be triggered either by intra-ring processes u or by inter-ring tunneling T. Eventually, the time evolution of the chiral current is easily found to be

$$\frac{d}{dt} J_{\text{chir}} = i\frac{2\sqrt{3}}{\hbar} T_\parallel T(a_1^\dagger b_1 + a_{-1} b_{-1}^\dagger - a_1 b_1^\dagger - a_{-1}^\dagger b_{-1}).$$

This equation confirms the intuitive fact that the angular momentum difference between the two rings cannot evolve in time if the inter-ring tunneling parameter T tends to zero.

As already noticed, the diagonal Hamiltonian (6) and the dynamics of physical observables we have presented are featured by two characteristic frequencies ω and Ω which, in the limit $T \to 0$, turn out to be equal. Different choices of parameters $(T_\parallel, u, T)$ result in different physical regimes, an aspect that will be discussed in the next section.

V. VORTEXLIKE EXCITATIONS AND CURRENT DYNAMICS

With reference to the double trimer, in the semiclassical picture, the expectation values of momentum-mode operators (expressed in terms of complex order parameters) can be written as

$$a_1 = \sqrt{n_1} e^{i\phi_1}, \quad a_{-1} = \sqrt{n_{-1}} e^{i\phi_{-1}},$$
$$b_1 = \sqrt{m_1} e^{i\psi_1}, \quad b_{-1} = \sqrt{m_{-1}} e^{i\psi_{-1}}.$$

In this section we show how different initial conditions (i.e., *moduli* and *phases* of the aforementioned operators at $t = 0$) together with different choices of parameters $T_\parallel, u$, and T lead to different dynamical regimes. The explicit solutions of Heisenberg equations giving the time evolution of excited populations $[n_{\pm 1}(t)$ and $m_{\pm 1}(t)]$ and of the rung current $J_\perp(t)$ can be found in the Supplemental Material [42]. Figure 2 sketches the five different initial conditions we will focus on.

(a) No initial excitations. If, at $t = 0, n_1 = n_{-1} = m_1 = m_{-1} = 0$, meaning that no excitations are present in the initial state, as time goes on, excitation pairs are periodically created and annihilated according to the relations

$$n_{\pm 1}(t) = m_{\pm 1}(t) = \frac{1}{2}\frac{u^2}{\hbar^2}\left[\frac{\sin^2(\omega t)}{\omega^2} + \frac{\sin^2(\Omega t)}{\Omega^2}\right].$$

This example clearly shows how a nonzero on-site repulsive term u determines fluctuations of the vacuum state $|n_1, n_{-1}, m_1, m_{-1}\rangle = |0,0,0,0\rangle$. Chiral and rung currents are identically zero.

The plots of $n_1(t)$ and $m_1(t)$, up to quantum fluctuations, show the periodic tunneling of the weakly populated vortex between the two rings, while the plots of $n_{-1}(t)$ and $m_{-1}(t)$ show the fluctuations of the vacuum state. Notice that chiral and rung currents' phases are permanently shifted of $\pi/2$, one being maximum (or minimum) when the other is zero. They somehow play a complementary role, analogous to that of position and momentum in a harmonic oscillator. This

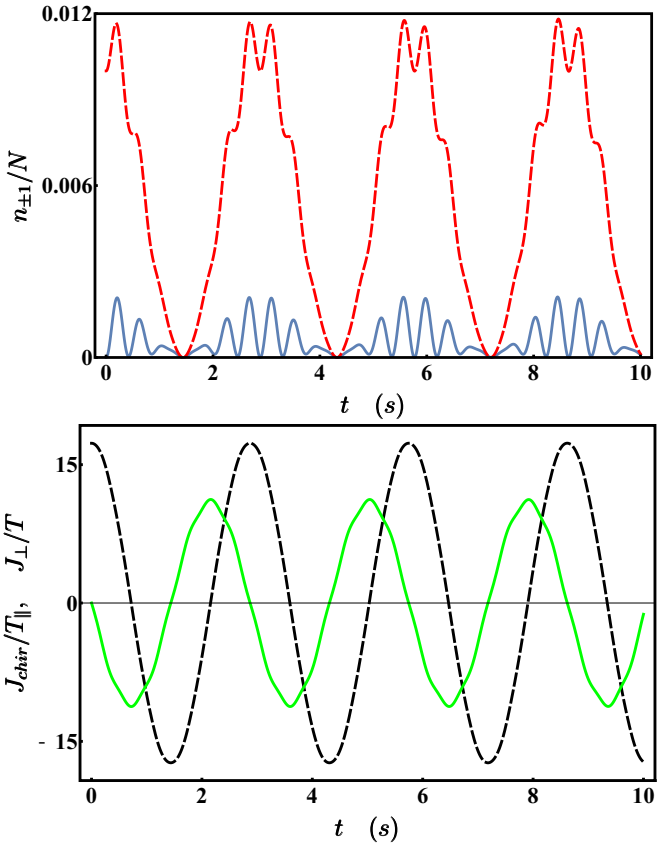

FIG. 3. Population and current dynamics for $T_\parallel = 2, U = 0.01, T = 1, \hbar = 1, N = 1000, n_1(0) = 10$, and $n_{-1}(0) = m_{\pm1}(0) = 0$. Top: $n_1(t)$ corresponds to the red dashed line, while $n_{-1}(t)$ corresponds to the blue solid line. $m_1(t)$ and $m_{-1}(t)$ feature the same behavior but are shifted by a semiperiod. Bottom: $J_{\text{chir}}(t)$ is depicted by the black dashed line, and $J_\perp(t)$ is shown by the green solid line.

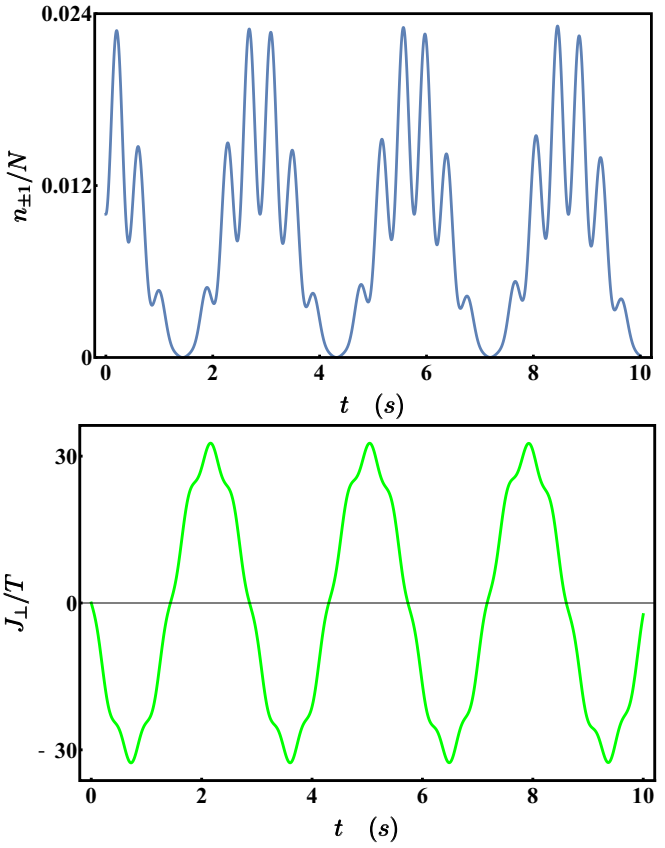

FIG. 4. Population and current dynamics for $T_\parallel = 2, U = 0.01, T = 1, \hbar = 1, N = 1000, n_1(0) = n_{-1}(0) = 10$, and $m_{\pm1}(0) = 0$. Since the tunneling process always involves *pairs* of bosons, there cannot be momentum transfer between the two rings; hence, chiral current is identically zero. $m_1(t)$ and $m_{-1}(t)$ feature the same behavior of $n_{\pm1}(t)$ but are shifted by a semiperiod.

statement is exact in the limit $u \to 0$, a case where the expressions of chiral and rung currents simplify as follows:

$$J_{\text{chir}}(t) = \sqrt{3} n_1(0) T_\parallel \cos\left(\frac{2tT}{\hbar}\right),$$

$$J_\perp(t) = -n_1(0) T \sin\left(\frac{2tT}{\hbar}\right).$$

Notice that the bigger the value of parameter T is, the wider the oscillations of the rung current are, and the higher the frequencies of J_{chir} and $J_\perp$ are. In short, a big value of T is linked to a fast and efficient transfer of bosons between the two rings.

The presence of a nonzero on-site repulsion is responsible for the periodic creation and annihilation of excited bosons pairs, which correspond to the high-frequency ripple in $n_{\pm1}(t), m_{\pm1}(t)$, and $J_\perp(t)$ (see Fig. 3). As a consequence, the bigger the value of u is, the wider the high-frequency oscillations of excited populations is (and the smaller their period is). This is a crucial point in order to obtain a both realistic and reliable description of the system: the global maximum of the excited populations must always be much less than the total number of bosons present in the system; otherwise, the Bogoliubov approximation is invalidated, and the model's predictions turn unphysical. According to the analysis we have carried out, the Bogoliubov approximation ceases to be valid for relatively small values of $U/T_\parallel$ and certainly *before* approaching Mott's lobes borders [43].

Moreover, it is interesting to notice that the inter-ring tunneling parameter T also affects the amplitude of excited-population oscillations and, when it approaches a certain upper limiting value, leads to dynamical instability. This issue will be deepened in next section.

(b) Weak vortex and equal weak antivortex in one ring, with no excitations in the other ring. If, at $t = 0, m_1 = m_{-1} = 0$ but $n_1 = n_{-1} \neq 0$, meaning that the initial state exhibits a balanced weak vortex-antivortex pair, as time goes on, excited bosons periodically tunnel from the first ring to the second ring and vice versa, giving place to a periodic rung current. Notice that the chiral current is identically zero, as the inter-ring tunneling process always involves *pairs* of bosons, as depicted in Fig. 4.

In regard to the population time evolution, it is possible to recognize a low-frequency component which corresponds to the periodic tunneling of excited bosons between the two rings and a high-frequency component which corresponds to quantum fluctuations of the vacuum state, which in turn are caused by a nonvanishing u. In this respect, notice that the on-site repulsion term u is associated with two-boson processes

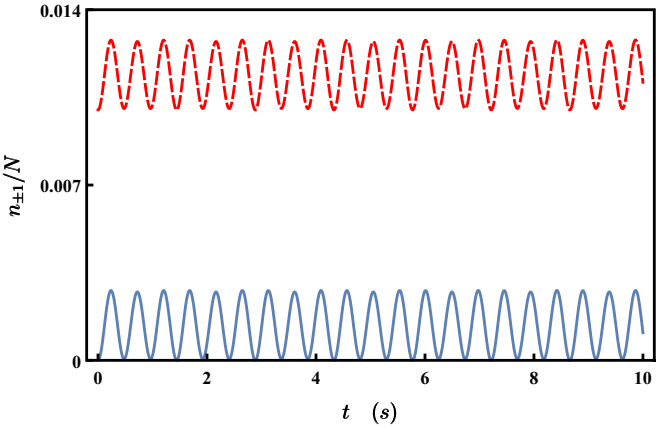

FIG. 5. Populations dynamics for $T_\parallel = 2$, $U = 0.01$, $T = 1$, $\hbar = 1$, $N = 1000$, $n_1(0) = m_1(0) = 10$, $n_{-1}(0) = m_{-1}(0) = 0$, and $\phi_1 = \psi_1 = 0$. $n_1(t)$ corresponds to the red dashed line, while $n_{-1}(t)$ corresponds to the blue solid line. As the tunneling is suppressed, $m_1(t)$ and $m_{-1}(t)$ feature the same behavior (fluctuations) as $n_1(t)$ and $n_{-1}(t)$, respectively. The chiral and the rung currents are identically zero.

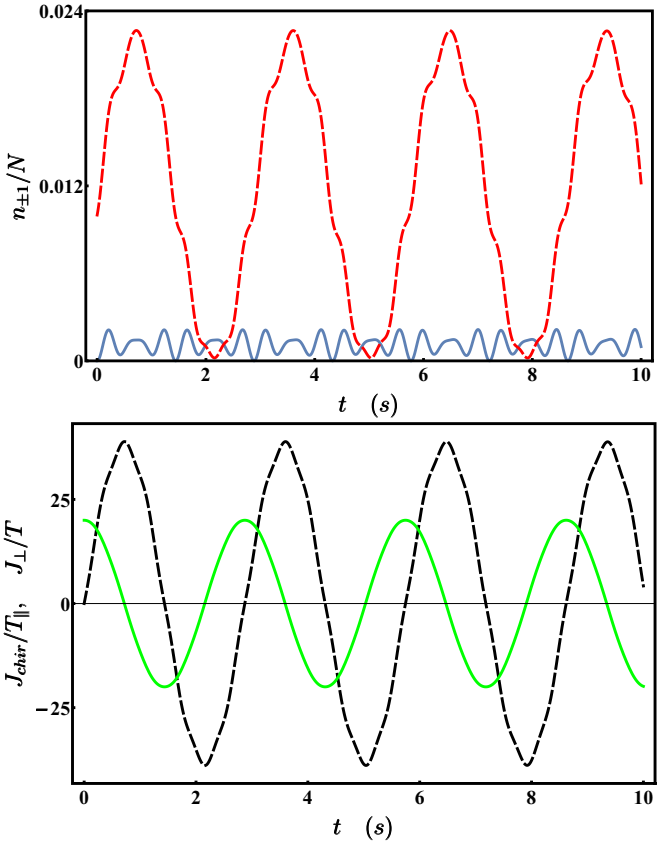

FIG. 6. Population and current dynamics for $T_\parallel = 2$, $U = 0.01$, $T = 1$, $\hbar = 1$, $N = 1000$, $n_1(0) = m_1(0) = 10$, $n_{-1}(0) = m_{-1}(0) = 0$, and $\psi_1 = 0$ but $\phi_1 = \frac{\pi}{2}$. Top: $n_1(t)$ corresponds to the red dashed line, while $n_{-1}(t)$ is depicted by the blue solid line. $m_{-1}(t)$ features exactly the same behavior as $n_{-1}(t)$, while $m_1(t)$ is shifted by a semiperiod with respect to $n_1(t)$. Apart from quantum fluctuations, one can notice that the weakly populated vortex with $k = +1$ periodically *completely* transfers from one ring to the other and vice versa. Bottom: Chiral current (in black) and rung current (in green).

$a_1^\dagger a_{-1}^\dagger$, $a_1 a_{-1}$, $b_1^\dagger b_{-1}^\dagger$, and $b_1 b_{-1}$, where the momentum in each single ring is indeed conserved.

(c) Two equal weak vortices in the two rings. Let us assume that $n_{-1}(0) = m_{-1}(0) = 0$ and that $n_1(0) = m_1(0) \neq 0$. This is a very interesting situation because the dynamics of our system inherently depends on the initial *phase difference* $\phi_1(0) - \psi_1(0)$. If this difference is zero, then the inter-ring tunneling process is suppressed, and up to quantum fluctuations, each ring always hosts the same number of excited bosons. As a consequence, chiral and rung currents are identically zero (see Fig. 5). Conversely, a nonvanishing phase difference is responsible for a periodic transfer of excited bosons from one ring to the other and vice versa (see Fig. 6). Hence, by observing $n_1(t)$ and $m_1(t)$ one can infer information about the *phases* of the two weakly populated vortices in the two rings. In this sense, the collective behavior which emerges in such a configuration can be used as a quantum interferometer.

(d) Weak vortex in one ring and equal (and opposite) weak antivortex in the other ring. Let us assume that $n_1(0) = m_{-1}(0) \neq 0$ and that $n_{-1}(0) = m_1(0) = 0$. Apart from quantum fluctuations (which correspond, as usual, to the high-frequency ripple in Fig. 7) excited bosons periodically tunnel from one ring to the other and vice versa. Remarkably, at each time, there are as many bosons which tunnel from ring A to ring B as bosons which tunnel from ring B to ring A. As a consequence, there is a continuous momentum transfer between the two rings, i.e., a periodic J_{chir}, but due to the symmetry of this tunneling process, $J_\perp$ is identically zero (see Fig. 7).

A. Towards instability

The diagonalization scheme presented in Sec. IV shows that there are some *constraints* on generalized rotation angles θ_a and θ_b [see Eq. (5)]. The same constraints also recur in the expression of diagonal Hamiltonian (6). Recalling that $T_\parallel$, u, and T are, by definition, non-negative numbers, all the diagonalization schemes and the dynamical results that we have presented so far are well defined iff $T < \frac{3}{2}T_\parallel$. If the inter-ring tunneling parameter T becomes large enough to approach the limiting value $\frac{3}{2}T_\parallel$, one can observe the spectral collapse, meaning that the separation between subsequent energy levels tends to zero (see Fig. 8).

In this respect, one should recall that diagonal Hamiltonian $\hat{\mathcal{H}}$ is, up to a constant term E_0, the sum of *four* harmonic oscillators, two of them having frequency Ω and the others having frequency ω [see Eqs. (4) and (6)]. As a consequence, two integer quantum numbers $n = n_1 + n_{-1}$ and $m = m_1 + m_{-1}$ are enough to label the energy levels of the system,

$$\hat{\mathcal{H}} = E_0 + \hbar\Omega\,(n+1) + \hbar\omega\,(m+1).$$

Of course an energy level labeled by quantum numbers (n,m) is $(n+1)(m+1)$ times degenerate. This is the number of eigenstates $|n_1,n_{-1},m_1,m_{-1}\rangle$ associated with a given energy. Figure 8 clearly shows that, if $T \to 0$, then $\Omega \to \omega$, meaning that one has the spectrum of a harmonic oscillator of frequency ω whose levels are $(m+3)!/(m!\,3!)$ times degenerate. Figure 8

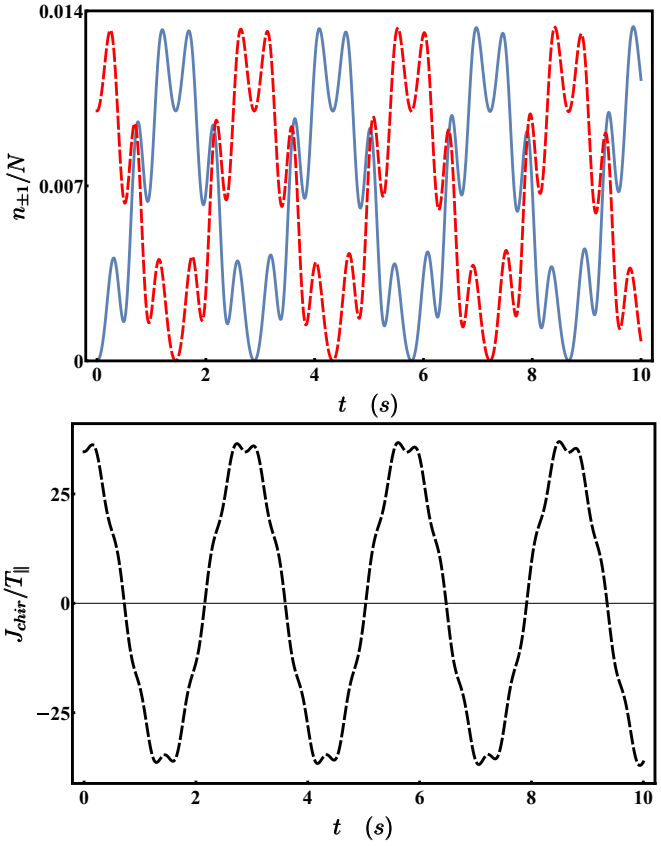

FIG. 7. Population and current dynamics for $T_\parallel = 2, U = 0.01, T = 1, \hbar = 1, N = 1000, n_1(0) = m_{-1}(0) = 10$, and $n_{-1}(0) = m_1(0) = 0$. n_1 and m_{-1} (dashed red line) have the same time evolution, and so do m_1 and n_{-1} (blue solid line). The rung current is identically zero.

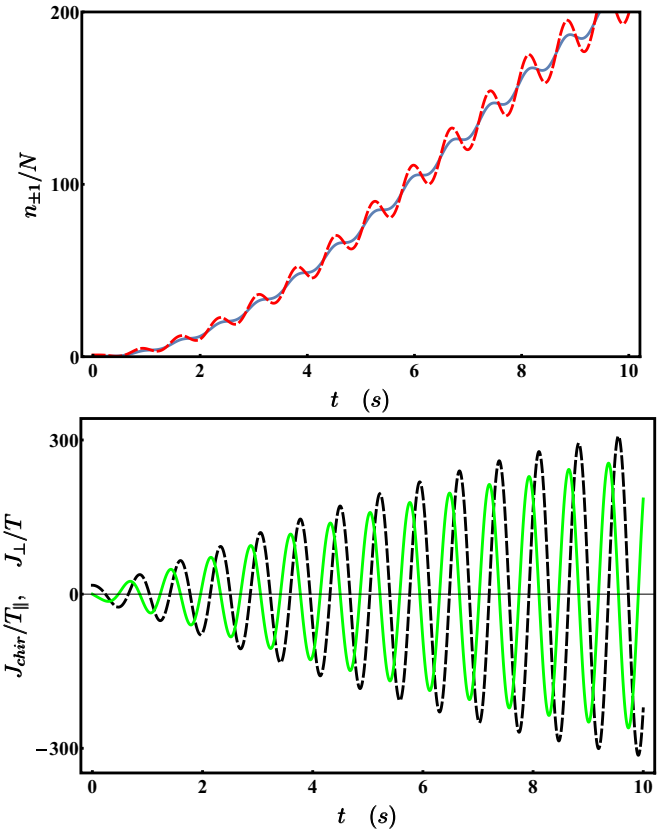

FIG. 9. Populations and currents dynamics for $T_\parallel = 2, U = 0.01, T = 2.999, \hbar = 1, N = 1000, n_1(0) = 10$, and $n_{-1}(0) = m_{\pm1}(0) = 0$. Top: $n_1(t)$ corresponds to the red dashed line, and $n_{-1}(t)$ is depicted by the blue solid line. $m_1(t)$ and $m_{-1}(t)$ essentially feature the same diverging behavior. The number of excited bosons rapidly increases and soon becomes nonphysical. Bottom: chiral (black dashed line) and rung (green solid line) currents exhibit a divergence too.

illustrates well the spectral collapse of (the energy levels of) the Ω-dependent harmonic oscillator for $T \to \frac{3}{2}T_\parallel$.

In regard to excited populations, approaching the border of the *stability* region, one observes that the numbers of excited bosons feature a *diverging* behavior, as Fig. 9 clearly depicts. This circumstance is not just a mathematical accident but serves to set the validity range of our model. Moreover, since the spectral collapse of the energy levels and the divergence of physical observables typically marks the appearance of unstable regimes, this phenomenology suggests the presence of a dynamical phase transition [29]. A well-known example is supplied by the BH ring model with attractive bosons where the interplay of the hopping parameter with the negative interaction can cause the spectral collapse [34]. In this respect, we emphasize how the presence of the inter-ring boson exchange described by T allows one to trigger unstable behaviors in the current model. The case $T > 3T_\parallel/2$ will be explored in a separate paper.

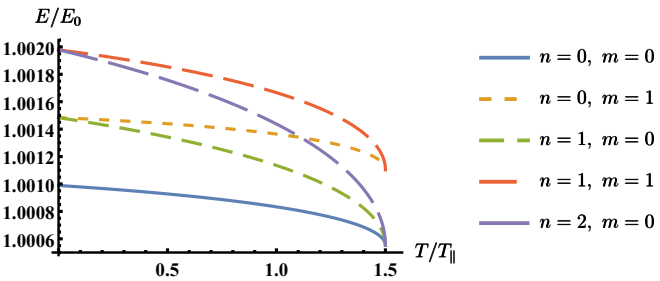

FIG. 8. Energy levels as a function of the intertunneling parameter T. When $T = 0$, the rings are decoupled; when $T \to \frac{3}{2}T_\parallel$, there is spectral collapse with respect to the first generalized harmonic oscillator.

B. Instability in a general double ring

The limiting condition $T < 3T_\parallel/2$ has been derived with reference to the double trimer. Nevertheless, it is possible to derive an analogous stability condition for a double ring which features a general number of sites M_s. Considering formula (2), one notices that each sub-Hamiltonian $\hat{H}_k$ features two characteristic frequencies,

$$\omega_k = \frac{1}{\hbar}\sqrt{(2T_\parallel C_k + 2u)2T_\parallel C_k}, \tag{9}$$

$$\Omega_k = \frac{1}{\hbar}\sqrt{(2T_\parallel C_k - 2T)(2T_\parallel C_k + 2u - 2T)}, \tag{10}$$

where $C_k := 1 - \cos(2\pi k/M_s)$. In passing, can observe that, choosing $M_s = 3$ and $k = 1$, one reobtains characteristic frequencies (7) and (8). Recalling that $T_\parallel$, u, and T are *positive* parameters, the stability condition is given by

$$2T_\parallel C_k - 2T > 0,$$

which results in

$$T < T_\parallel C_k.$$

Since C_k is a monotonically increasing function for $0 < k < (M_s - 1)/2$, the limiting value of T is found for $k = 1$, i.e.,

$$T < T_\parallel \left[1 - \cos\left(\frac{2\pi}{M_s}\right)\right].$$

In other words, whatever the number of sites in the system, the sub-Hamiltonian which collapses first (due to an increase in T) is always $\hat{H}_1$.

As already mentioned, our model can also describe the dynamics of systems which feature an *attractive* interaction $U < 0$, provided that the condition that $|U|/T$ is small enough is fulfilled, thus guaranteeing that bosons are superfluid and delocalized [34]. For such systems, two conditions,

$$u > T_\parallel \left[\cos\left(\frac{2\pi}{M_s}\right) - 1\right],$$
$$T < T_\parallel \left[1 - \cos\left(\frac{2\pi}{M_s}\right)\right] + u,$$

ensure that the spectrum is real and discrete. A systematic exploration of the attractive regime includes the case when $|U|/T$ is large. In this case the formation of solitonlike quantum states characterized by boson localization (see, for example, [44–46]), typically occurring in the single-ring geometry, is expected. The quantum study of the interaction between solitons on different rings and in complex geometries [47,48] will be developed elsewhere along the lines of Ref. [49].

VI. CONCLUDING REMARKS

In this work we have focused on the BH two-ring ladder. In Sec. II we showed that, moving to the momentum-mode picture and performing the well-known Bogoliubov approximation, the system Hamiltonian, up to a constant term E_0, decouples in $(M_s - 1)/2$ independent Hamiltonians $\hat{H}_k$, one for each *pair* of momentum modes. In Sec. III, we proved that each Hamiltonian $\hat{H}_k$ belongs to a dynamical algebra so(2,3). This property has provided not only an effective diagonalization scheme but also the possibility of computing the conserved quantity in the system and its dynamical equations.

Section IV was devoted to applying our solution scheme to a simple and yet very interesting example: the double twin trimer where the ground state features a $r = 0$ mode macroscopically occupied. After finding the explicit expression of its spectrum, we showed that the excitations of the system indeed can be seen as weakly populated vortices. Then we introduced some significant physical observables, which are currently used in the literature [18,41] and computed their time evolution thanks to the closure property of the algebraic framework.

The derived dynamical equations have highlighted the fundamental processes which happen in the system. We have also noticed that, while some "global" observables (namely, N_* and $J_\perp$) can be written as elements of the dynamical algebra so(2,3), in order to have a more detailed description of microscopic physical processes (e.g., the time evolution of boson populations) it is necessary to perform the immersion of the algebra so(2,3) in the larger 15-dimensional algebra so(2,4). It is within this larger algebraic framework that the dynamics of all the observables typically used in literature takes place.

Finally, in Sec. V, we explored the system evolution for different choice of parameters and initial conditions. In particular, we explicitly described the vacuum-state fluctuations and the coherent time evolution of the rung and chiral currents. Also, we found a configuration where a different choice in the initial *phase difference* of the excitation modes in the two rings allows us to completely inhibit the boson inter-ring exchange. In conclusion, we have analyzed the stability region of the system and noticed that, for $T \to \frac{3}{2}T_\parallel$, the system turns out to be unstable, hinting at the possible presence of a dynamical phase transition. This issue, the study of strongly interacting attractive bosons, and the study of the excitation dynamics for the macroscopic modes $r \neq 0$ (vortex configurations) will be explored in a future work.

APPENDIX A

The two terms with the triple summation can be simplified considering just the addends which include at least two r-mode operators:

$$\sum_{p,q,k=1}^{M_s} a^\dagger_{q+k} a^\dagger_{p-k} a_q a_p \approx n_r(n_r - 1) + 4n_r \sum_{k\neq r} n_k + (a_r)^2 \sum_{k\neq r} a^\dagger_{r+k} a^\dagger_{r-k} + (a^\dagger_r)^2 \sum_{k\neq r} a_{r+k} a_{r-k}.$$

Of course, the same reasoning holds also for the second ring, i.e., for the term proportional to U_b.

According to the well-known Bogoliubov approximation, a mode operator relevant to a macroscopically occupied mode can be declassed to a complex number whose phase can be arbitrarily chosen to be zero. Performing the substitutions $a^\dagger_r \to \sqrt{n_r}$, $a_r \to \sqrt{n_r}$, $b^\dagger_r \to \sqrt{m_r}$, $b_r \to \sqrt{m_r}$ and writing n_r as $N - \sum_{k\neq r} n_k$ and m_r as $M - \sum_{k\neq r} m_k$, the Hamiltonian assumes the following form:

$$\hat{H} = \hat{H}_a + \hat{H}_b + \hat{H}_\perp,$$

where

$$\hat{H}_a = -2T_a \left[N\cos(a\tilde{r}) + \sum_{k\neq r} (\cos(a\tilde{k}) - \cos(a\tilde{r}))n_k\right] + \frac{u_a}{2}\left[N - 1 + \sum_{k\neq 0}(n_{r+k} + n_{r-k} + a^\dagger_{r+k} a^\dagger_{r-k} + a_{r+k} a_{r-k})\right],$$

$$\hat{H}_b = -2T_b\left[M\cos(a\tilde{r}) + \sum_{k\neq r}(\cos(a\tilde{k}) - \cos(a\tilde{r}))m_k\right] + \frac{u_b}{2}\left[M - 1 + \sum_{k\neq 0}(m_{r+k} + m_{r-k} + b^\dagger_{r+k}b^\dagger_{r-k} + b_{r+k}b_{r-k})\right],$$

$$\hat{H}_\perp = -2T\sqrt{NM} - T\sqrt{\frac{M}{N}}\sum_{k\neq r} n_k - T\sqrt{\frac{N}{M}}\sum_{k\neq r} m_k + \frac{T}{2}\sum_{k\neq r}(a_{r+k}b^\dagger_{r+k} + a^\dagger_{r+k}b_{r+k} + a_{r-k}b^\dagger_{r-k} + a^\dagger_{r-k}b_{r-k}).$$

APPENDIX B

Here we give the defining commutators of our ten-dimensional algebra. In the main text, we already mentioned that $\{A_+, A_-, A_3\}$ generate an su(1,1) algebra and $\{B_+, B_-, B_3\}$ do too. Concerning operators $\{S_+, S_-, A_3 - B_3\}$, they generate an su(2) algebra, the latter being marked by commutators: $[S_+, S_-] = 2(A_3 - B_3)$, $[S_\pm, A_3 - B_3] = \mp S_\pm$. Operators $\{K_+, K_-, A_3 + B_3\}$ generate another su(1,1) algebra, the defining commutators being $[K_+, K_-] = -2(A_3 + B_3)$, $[K_\pm, A_3 + B_3] = \mp K_\pm$. After recognizing the presence of these four subalgebras, we give the commutation relations between the elements of the various subalgebras. Any element A_i commutes with all elements B_j, i.e., $[A_i, B_j] = 0$, with $i, j = +, -, 3$. Moreover,

$$\begin{aligned}
&[A_+, S_+] = 0, \quad [A_+, S_-] = -K_+, \quad [A_+, K_+] = 0,\\
&[A_+, K_-] = -S_+, \quad [A_-, S_+] = K_-, \quad [A_-, S_-] = 0,\\
&[A_-, K_+] = S_-, \quad [A_-, K_-] = 0,\\
&[A_3, S_\pm] = \pm\frac{1}{2}S_\pm, \quad [A_3, K_\pm] = \pm\frac{1}{2}K_\pm,\\
&[B_+, S_+] = -K_+, \quad [B_+, S_-] = 0, \quad [B_+, K_+] = 0,\\
&[B_+, K_-] = -S_-, \quad [B_-, S_+] = 0, \quad [B_-, S_-] = K_-,\\
&[B_-, K_+] = S_+, \quad [B_-, K_-] = 0,\\
&[B_3, S_\pm] = \mp\frac{1}{2}S_\pm, \quad [B_3, K_\pm] = \pm\frac{1}{2}K_\pm,\\
&[S_+, K_+] = 2A_+, \quad [S_+, K_-] = -2B_-,\\
&[S_-, K_+] = 2B_+, \quad [S_-, K_-] = -2A_-.
\end{aligned}$$

APPENDIX C

The explicit expressions of the unitary transformations have been computed using the well-known Campbell-Baker-Hausdorf formula

$$e^X\, Y\, e^{-X} = \sum_{k=0}^{+\infty}\frac{1}{k!}[X, Y]_k.$$

As we are working within an algebraic framework, the algebra's closure property guarantees that any commutator of two algebra elements is still an algebra element. Generalized rotation angles φ, ξ, θ_a, and θ_b are computed by imposing the nullification of nondiagonal operators. Their expression is

$$\begin{aligned}
\tan\varphi &= \frac{2T(\gamma_{a,k} + \gamma_{b,k})}{(u_a + u_b)(u_a - u_b) - (\gamma_{a,k} + \gamma_{b,k})(\gamma_{a,k} - \gamma_{b,k}),}\\
\tanh\xi &= \frac{2T(u_b - u_a)}{\left(u_a^2 - u_b^2 - \gamma_{a,k}^2 + \gamma_{b,k}^2\right)\sqrt{1+\chi}},\\
\chi &= \frac{4T^2(\gamma_{a,k} + \gamma_{b,k})^2}{\left(u_a^2 - u_b^2 - \gamma_{a,k}^2 + \gamma_{b,k}^2\right)^2},\\
\tanh\theta_a &= \frac{c_2}{c_1}, \quad \tanh\theta_b = \frac{c_4}{c_3}.
\end{aligned}$$

Coefficients c_1, c_2, c_3, and c_4 have the following expressions:

$$\begin{aligned}
c_1 &= (u_a - u_b)\sinh\xi\sin\varphi + (\gamma_{a,k} + \gamma_{b,k})\cosh\xi - 2T\sin\varphi + (\gamma_{a,k} - \gamma_{b,k})\cos\varphi,\\
c_2 &= 2T\sinh\xi\cos\varphi + (\gamma_{a,k} - \gamma_{b,k})\sinh\xi\sin\varphi + \cosh\xi(u_a + u_b) + (u_a - u_b)\cos\varphi,\\
c_3 &= (u_a - u_b)\sinh\xi\sin\varphi + (\gamma_{a,k} + \gamma_{b,k})\cosh\xi + 2T\sin\varphi - (\gamma_{a,k} - \gamma_{b,k})\cos\varphi,\\
c_4 &= 2T\sinh\xi\cos\varphi + (\gamma_{a,k} - \gamma_{b,k})\sinh\xi\sin\varphi + \cosh\xi(u_a + u_b) - (u_a - u_b)\cos\varphi.
\end{aligned}$$

APPENDIX D

The 15 generators of the algebra so(2,4) are

$$\begin{aligned}
&A_+ = a_1^\dagger a_{-1}^\dagger, \quad A_- = A_+^\dagger, \quad A_3 = \tfrac{1}{2}(n_1 + n_{-1} + 1),\\
&B_+ = b_1^\dagger b_{-1}^\dagger, \quad B_- = B_+^\dagger, \quad B_3 = \tfrac{1}{2}(m_1 + m_{-1} + 1),\\
&Q_+ = a_1^\dagger b_1, \quad Q_- = Q_+^\dagger \quad G_+ = a_{-1}^\dagger b_1^\dagger, \quad G_- = G_+^\dagger,\\
&H_+ = a_1^\dagger b_{-1}^\dagger, \quad H_- = H_+^\dagger \quad R_+ = a_{-1}^\dagger b_{-1}, \quad R_- = R_+^\dagger,\\
&T = \tfrac{1}{2}[(n_1 - n_{-1}) - (m_1 - m_{-1})].
\end{aligned}$$

The relevant Casimir operator is

$$\begin{aligned}
C = {} & A_3^2 + B_3^2 + \tfrac{1}{2}\,T^2\\
& + \tfrac{1}{2}[Q_+Q_- + Q_-Q_+ + R_+R_- + R_-R_+]\\
& - \tfrac{1}{2}[A_+A_- + A_-A_+ + B_+B_- + B_-B_+ G_+G_-\\
& + G_-G_+ + H_+H_- + H_-H_+],
\end{aligned}$$

which can be written in the standard form $C = \frac{3}{2}K_4(K_4 + 2)$, where $K_4 = (n_1 - n_{-1} + m_1 - m_{-1} - 2)/2$ represents the total angular momentum. This shows how the algebra so(2,4) again features the total angular momentum as a conserved quantity.

[1] M. K. Olsen and A. S. Bradley, Phys. Rev. A **91**, 043635 (2015).
[2] B. T. Seaman, M. Krämer, D. Z. Anderson, and M. J. Holland, Phys. Rev. A **75**, 023615 (2007).
[3] S. C. Caliga, C. J. E. Straatsma, A. A. Zozulya, and D. Z. Anderson, New J. Phys. **18**, 015012 (2016).
[4] R. A. Pepino, J. Cooper, D. Z. Anderson, and M. J. Holland, Phys. Rev. Lett. **103**, 140405 (2009).
[5] A. Benseny, S. Fernández-Vidal, J. Bagudà, R. Corbalán, A. Picón, L. Roso, G. Birkl, and J. Mompart, Phys. Rev. A **82**, 013604 (2010).
[6] I. Bloch, J. Dalibard, and S. Nascimbène, Nat. Phys. **8**, 267 (2012).
[7] R. P. Feynman, Int. J. Theor. Phys. **21**, 467 (1982).
[8] Y.-J. Lin, R. L. Compton, K. Jimenez-Garcia, J. V. Porto, and I. B. Spielman, Nature (London) **462**, 628 (2009).
[9] M. Atala, M. Aidelsburger, M. Lohse, J. T. Barreiro, B. Paredes, and I. Bloch, Nat. Phys. **10**, 588 (2014).
[10] C.-C. Chien, S. Peotta, and M. Di Ventra, Nat. Phys. **11**, 998 (2015).
[11] N. Goldman, J. Budich, and P. Zoller, Nat. Phys. **12**, 639 (2016).
[12] L. Amico, A. Osterloh, and F. Cataliotti, Phys. Rev. Lett. **95**, 063201 (2005).
[13] D. Aghamalyan, L. Amico, and L. C. Kwek, Phys. Rev. A **88**, 063627 (2013).
[14] I. Lesanovsky and W. von Klitzing, Phys. Rev. Lett. **98**, 050401 (2007).
[15] A. Gallemí, A. M. Mateo, R. Mayol, and M. Guilleumas, New J. Phys. **18**, 015003 (2015).
[16] L. Amico, D. Aghamalyan, F. Auksztol, H. Crepaz, R. Dumke, and L. C. Kwek, Sci. Rep. **4**, 4298 (2014).
[17] E. Orignac and T. Giamarchi, Phys. Rev. B **64**, 144515 (2001).
[18] M. Piraud, F. Heidrich-Meisner, I. P. McCulloch, S. Greschner, T. Vekua, and U. Schollwock, Phys. Rev. B **91**, 140406 (2015).
[19] M. Di Dio, S. De Palo, E. Orignac, R. Citro, and M.-L. Chiofalo, Phys. Rev. B **92**, 060506 (2015).
[20] A. Tokuno and A. Georges, New J. Phys. **16**, 073005 (2014).
[21] S. Uchino, Phys. Rev. A **93**, 053629 (2016).
[22] T. Haug, L. Amico, R. Dumke, and L.-C. Kwek, arXiv: 1612.09109.
[23] R. Sachdeva, M. Singh, and T. Busch, Phys. Rev. A **95**, 063601 (2017).
[24] M. Rasetti, Int. J. Theor. Phys. **13**, 425 (1975).
[25] W.-M. Zhang, D. H. Feng, and R. Gilmore, Rev. Mod. Phys. **62**, 867 (1990).
[26] R. Kaushal and S. Mishra, J. Math. Phys. **34**, 5843 (1993).
[27] E. Celeghini, L. Faoro, and M. Rasetti, Phys. Rev. B **62**, 3054 (2000).
[28] R. Franzosi, V. Penna, and R. Zecchina, Int. J. Mod. Phys. B **14**, 943 (2000).
[29] V. Penna, Phys. Rev. E **87**, 052909 (2013).
[30] E. Torrontegui, S. Martinez-Garaot, and J. G. Muga, Phys. Rev. A **89**, 043408 (2014).
[31] F. Lingua, G. Mazzarella, and V. Penna, J. Phys. B **49**, 205005 (2016).
[32] A. M. Rey, K. Burnett, R. Roth, M. Edwards, C. J. Williams, and C. W. Clark, J. Phys. B **36**, 825 (2003).
[33] K. Burnett, M. Edwards, C. W. Clark, and M. Shotter, J. Phys. B **35**, 1671 (2002).
[34] M. W. Jack and M. Yamashita, Phys. Rev. A **71**, 023610 (2005).
[35] A. I. Solomon, Y. Feng, and V. Penna, Phys. Rev. B **60**, 3044 (1999).
[36] R. Gilmore, *Lie Groups, Physics, and Geometry: An Introduction for Physicists, Engineers and Chemists* (Cambridge University Press, Cambridge, 2008).
[37] L. Casetti and V. Penna, J. Low Temp. Phys. **126**, 455 (2002).
[38] P. Buonsante, R. Franzosi, and V. Penna, J. Phys. A **42**, 285307 (2009).
[39] G. Arwas, A. Vardi, and D. Cohen, Sci. Rep. **5**, 13433 (2015).
[40] X. Han and B. Wu, Phys. Rev. A **93**, 023621 (2016).
[41] S. S. Natu, Phys. Rev. A **92**, 053623 (2015).
[42] See Supplemental Material at http://link.aps.org/supplemental/10.1103/PhysRevA.96.013620 for the time evolution of excited populations and of the rung current is derived.
[43] F. E. A. dos Santos and A. Pelster, Phys. Rev. A **79**, 013614 (2009).
[44] P. Buonsante, V. Penna, and A. Vezzani, Phys. Rev. A **72**, 043620 (2005).
[45] G. M. Kavoulakis, Phys. Rev. A **67**, 011601(R) (2003).
[46] R. Kanamoto, H. Saito, and M. Ueda, Phys. Rev. A **73**, 033611 (2006).
[47] P. Buonsante, R. Burioni, D. Cassi, and A. Vezzani, Phys. Rev. B **66**, 094207 (2002).
[48] P. Buonsante, V. Penna, and A. Vezzani, Phys. Rev. B **70**, 184520 (2004).
[49] S. M. Cavaletto and V. Penna, J. Phys. B **44**, 115308 (2011).